DE GRUYTER OPEN

Stable phase CdS nanoparticles for optoelectronics: A study on surface morphology, structural and optical characterization

SURESH KUMAR[1*], J.K. SHARMA[2]

[1]Department of Applied Sciences and Humanities, Maharishi Markandeshwar University, Sadopur, Ambala-134007, Haryana, India

[2]Department of Physics, Maharishi Markandeshwar University, Mullana, Ambala-133207, India

This work presents a study on the surface morphology, structure and optical behavior of stable phase cadmium sulphide (CdS) nanoparticles synthesized via co-precipitation technique. Scanning electron microscopy (SEM) analysis has been employed to study a cluster formation in the aggregated nanoparticles. An image analysis approach using ImageJ has been used to measure the size of nanoparticles from the SEM micrographs. Fourier transform infrared spectroscopic (FT-IR) analysis identified absorption peaks of Cd–S stretching along with moisture content. X-ray diffraction (XRD) analysis showed that CdS nanoparticles crystallized in wurtzite structure with a preferential orientation along (0 0 2) plane. The particle size, microstrain and lattice constants have been evaluated using XRD data. The lattice parameters of these nanoparticles were found to be shorter than the bulk value which led to lattice contraction. The optical absorption study showed a blue shift in the fundamental absorption edge indicating a quantum size effect.

Keywords: *CdS nanoparticles; surface morphology; structural analysis; optical absorption; quantum size effect*

1. Introduction

Recent developments in nanotechnology proved that many novel devices of the future will be based on the properties of nanomaterials [1–4]. Presently, nanomaterials are produced in various nanoforms, such as quantum dots, nanoparticles, nanowires, nanotubes, nanoprisms, nanofilms etc., by employing top-down and bottom-up approaches [4, 5]. The nanoforms of semiconductor materials have received great attention due to their unique properties and potential applications. They exhibit entirely different physicochemical properties than their bulk counterparts, due to increased relative surface area and quantum confinement [4, 6]. The particle size and morphology of these nanomaterials can be easily changed and hence, enhancement in their various properties, such as reactivity, strength, optoelectronic,

electrical, magnetic behavior etc., and finally their potential applications, can be achieved. Binary semiconductors (group II – VI) in various nanoforms have many scientific and technological applications [7–9]. CdS is a promising binary II – VI semiconductor used in variety of optoelectronic applications, including solar cell windows, laser communication, photoconductors, field effect transistors, sensors, photocatalysts, biological indicators, light emitting diodes, etc. [9–12]. It is a wide band gap semiconductor lightly soluble in water and highly soluble in acid. In nature, it is found in greenockite (wurtzite), hawleyite (zinc blende) and rocksalt mineral structures [6]. The zinc blende to wurtzite transformation involves a change in symmetry whereas wurtzite to rocksalt transformation involves not only a change in symmetry but also a change in the nearest neighbor atomic coordination from four to six [6]. The wurtzite (α-CdS) and zinc blende (β-CdS) forms are the most common crystal formation

---

of CdS having lattice parameters $a_{wz} = 4.137$ Å, $c_{wz} = 6.7144$ Å and $a_{zb} = 5.832$ Å, respectively [13]. The wurtzite form of CdS, due to its stable nature, has been preferred for the fabrication of devices. Therefore, more extensive studies on the nanoforms of CdS semiconductor and their various properties have been carried out. A variety of chemical routes to synthesize CdS nanoforms have been employed [6, 9, 14–22]. However, the co-precipitation technique is an important bottom-up approach for the synthesis of nanoparticles. It is simple, inexpensive, free from complex instrument handling and a low temperature processing technique [23]. It also has the potential advantage to prepare nanoparticles of relatively low cost, high purity and controlled morphology. It can be performed using a wide range of precursors with easy control over synthesis parameters, such as pH, temperature, time, stirring rate, concentration of reactants etc. The controlled variation of the synthesis parameters may lead to optimizing the size, geometry and morphology of the resulting nanoparticles.

This work reports the synthesis of CdS nanoparticles via co-precipitation technique without any capping agent. The present study is an effort to explore the physical and optical behavior of chemically synthesized stable phase CdS nanoparticles.

2. Experimental

2.1. Synthesis of CdS nanoparticles

All chemicals used in the synthesis were analytical grade products purchased from Merck, India and were used as received without further purification. The chemicals that were used for the synthesis of CdS nanoparticles were cadmium chloride anhydrous ($CdCl_2H_2O$) as the source of Cd^{2+} ions, thiourea ($CS(NH_2)_2$) as the source of S^{2-} ions and ammonia solution (NH_4OH) as the complexing agent to control precipitation. To prepare CdS nanoparticles, the equimolar (0.2 M) aqueous solutions of the reactants, cadmium chloride and thiourea were prepared using double distilled water (Millipore, 15 MΩ·cm) separately.

The ammonia solution (25 %) was added dropwise through a burette into 25 mL of cadmium chloride solution under slow stirring. It was added to dissolve the white precipitate of $Cd(OH)_2$ under constant magnetic stirring rate (300 rpm) till a clear transparent solution formed. Finally 25 mL aqueous solution of thiourea was mixed into it. The pH of the solution was stabilized at 10.5±0.1 by ammonia addition. The whole synthesis process was carried out under continuous stirring at temperature of 70±2 °C using a hot plate magnetic stirrer. Initially, as the reaction started the solution color gradually changed from transparent to light yellow, which suggested precipitation, and finally turned to dark yellow. To remove any type of unreacted chemicals or impurities, the precipitates were washed several times with double distilled water and finally collected by centrifugation process. The collected CdS precipitate was first dried in a glass desiccator to get CdS nanoparticles in powder form and then annealed in a muffle furnace at temperature of 300 °C for 3 hours.

2.2. Characterization techniques

The surface morphology of CdS nanoparticles has been studied using SEM (JEOL JSM- 6100) operated at 20 kV at a magnification of 14 000. An image processing approach using ImageJ programme has been also used to measure the particle size from 2D SEM images. Fourier transform infrared spectroscopy (FT-IR) measurement has been performed by Perkin Elmer 1600 FT-IR in the spectral range of 400 cm^{-1} to 4000 cm^{-1} in % T mode using KBr pellet technique. The X-ray powder diffraction (XRD) data was recorded using PANaytical's X'Pert-Pro diffractometer, with CuKα radiation ($\lambda = 1.5406$ Å), operating at 40 kV and 40 mA. The 2θ scanning range was from 10° to 60° in steps of 0.02°. The XRD data was further analyzed for baseline correction, fitting and peak parameters using Fityk-093 software. The optical absorption spectrum (210 nm to 1000 nm) was recorded using an UV-Vis-NIR Perkin Elmer Lambda 40 spectrophotometer.

3.   Results and discussion

3.1.   Surface morphology analysis

Scanning electron microscopy (SEM) micrograph (Fig. 1a) shows that CdS nanoparticles exist in flocks. These flocks are formed by infinite numbers of crystallites which aggregated densely. The formation of these compact flocks in CdS powder is due to homogeneous precipitation that occurs during the synthesis process followed by cluster growth of crystallites [9, 18]. These nanocrystallites are embedded in these clusters and acquire flake like shapes. In case of powder samples the shape, size and boundaries of particles are difficult to identify only using SEM images and hence, ImageJ programme was used for image analysis [24, 25]. Fig. 1b to Fig. 1d show 2D images transformed by following the image analysis procedure within ImageJ programme. The analysis of the SEM image was carried out in different steps such as setting a scale for 2D SEM image, removing noise using Gaussian blur filter, setting threshold (Fig. 1b) and detecting boundaries of the nanoparticles through binary image (Fig. 1c). Finally the binary image was subjected to automatic identification and counting the number of particles (Fig. 1d). The average size of nanoparticles estimated by the imageJ programme through the analyzing tool was found to be 16.3 nm.

3.2.   Fourier transform infrared analysis

Analyzing the FT-IR spectrum (Fig. 2), it has been observed that many absorption peaks and bands exist in the synesized CdS nanopowder (inset in Fig. 2) which belong to the molecular alignment of the elements. Normally Cd–S stretching frequency has been found in the lower wave number region, i.e. below 700 cm^{-1} [15]. In our CdS nanoparticles, a medium strong absorption peak at 651.62 cm^{-1} belonging to Cd–S stretching has been observed. The absorption peaks at 1074.86 cm^{-1} and 1165.35 cm^{-1} belong to C–N stretch/C=S of thiourea and the peak at 1373.13 cm^{-1} corresponds to tris-amine C–N stretch shared with C–O stretching. Moreover, the peaks at 2000.37 cm^{-1} and 2150.47 cm^{-1}
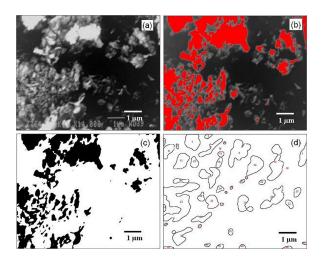

Fig. 1. (a) original 2D SEM micrographs, ImageJ processed images (b) threshold image after eliminating noise (c) binary image for boundary distribution and (d) final image employed to measure particle size.

also correspond to N=C stretch or isothiocynate (–NCS) which formed due to hydrolysis of thiourea during the synthesis [17, 26]. A weak doublet at 2923.61 cm^{-1} and 2853.01 cm^{-1} has been assigned to asymmetrical and symmetrical vibrations of CH group, respectively, while the asymmetric scissor deformation vibration exits at 1445.50 cm^{-1} [26]. The medium strong and broad absorption bands at 3428.98 cm^{-1} and 1629.96 cm^{-1} have been assigned to O–H stretching vibration of H$_2$O molecules [26]. Another weak absorption peak at 898.46 cm^{-1} belongs to O–H out of plane bending vibration of H$_2$O molecules. These vibrations have been observed because of the moisture content that exists in CdS nanoparticles even after thermal annealing. The existence of respective absorption peaks and bands in FT-IR spectrum confirms the presence of CdS molecules, the impurities traces, because of chemical reaction of different precursors used, and water molecules or hydroxide ions in the prepared nanoparticles.

3.3.   Structural characterization by X-ray diffraction

The presence of multiple diffraction peaks with the broad peak profile in the XRD spectrum (Fig. 3) can be attributed to the polycrystalline behavior
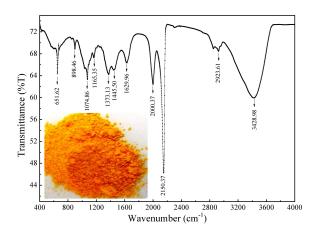
Fig. 2. FT-IR spectrum for CdS nanoparticles; the inset shows original CdS nanopowder.

of the synthesized CdS nanoparticles. Moreover, the diffused background on the XRD spectrum may be due to the amorphous character associated with disordered periodicity of lattice elements. This type of behavior is commonly observed in nanosized particles [14]. The comparison of XRD peak profile and the 2θ position of diffraction peaks (Table 1) with standard ASTM data confirms the wurtzite (α-CdS) crystal structure with the preferential orientation along (0 0 2) plane [10]. An additional peak at 2θ = 31.33° has also been detected which corresponds to hcp CdO [27]. This may point out that the synthesized CdS nanoparticles are rich in Cd content. The intensity of diffraction peaks (Table 1) has been observed to be low as compared to bulk CdS [10]. It is also observed that the positions of diffraction peaks for CdS nanoparticles shift to higher diffraction angles in comparison to bulk CdS. This may be due to lattice contraction which is expected to occur because of higher surface to volume ratio of nanoparticles [18]. The interplanar spacing 'd$_{hkl}$' values have been evaluated (Table 1) using Bragg's diffraction equation [9]. The smaller values of d$_{hkl}$ than the standard d$_{hkl}$ value also support the lattice contraction in the synthesized CdS nanoparticles. Williamson-Hall (W-H) plot (Fig. 4) has been used to evaluate the particle size (D$_v$) and microstrain (ε$_{hkl}$) as [28]:

$$\beta_{hkl} \cos \theta_{hkl} = \left(\frac{\lambda}{D_v} \right) + 4\varepsilon_{hkl} \sin \theta_{hkl} \qquad (1)$$

where β$_{hkl}$ is the integral peak width associated with Bragg angle (θ$_{hkl}$). The obtained values for D$_v$ and ε$_{hkl}$ are 15.23 nm and 6.93×10^{-3}, respectively. The particle size calculated from XRD analysis is in good agreement with those obtained from imageJ analysis of 2D SEM micrograph. The lattice constants (a and c) for the hexagonal structure have been determined using the relation [28] as:

$$\frac{1}{d_{hkl}} = \frac{4}{3} \left\{ \frac{h^2 + hk + k^2}{a^2} \right\} + \left(\frac{l^2}{c^2} \right) \qquad (2)$$

where (hkl) are Miller indices of the respective reflecting planes. The average values of a and c have been calculated as 4.081 Å and 6.662 Å respectively with an error approximation of ±0.001 Å. The lattice constants for the synthesized CdS nanoparticles were found to be less than standard values [10]. Thus it can be concluded that the lattice is contracted which may be due to the presence of defects like surface or interface stress, strain and dislocations, etc., associated with reduced size of nanoparticles [29].
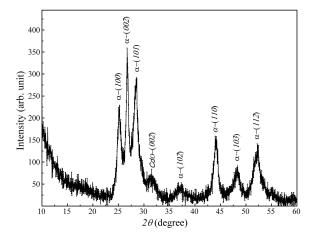

Fig. 3. XRD spectrum for CdS nanoparticles.

3.4. Optical characterization

One of the important features of semiconductor nanoparticles is their optical behavior. Today it is well known that as the particle size of a semiconductor decreases and approaches the size of Bohr exciton the optical band gap increases [9, 30, 31]. This can be observed as a shift in the absorption

Table 1. Structural parameters for CdS nanoparticles with corresponding standard values.

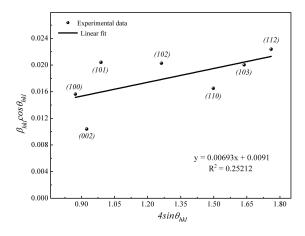| Observed values			Standard values			Miller planes
2θ [deg.]	d_{hkl} [Å]	Intensity	2θ [deg.]	d_{hkl} [Å]	Intensity	
25.17	3.535	60.72	24.85	3.582	59.21	(1 0 0)
26.74	3.331	100.00	26.55	3.357	42.68	(0 0 2)
28.44	3.135	79.94	28.23	3.160	100.00	(1 0 1)
37.10	2.421	13.75	36.68	2.439	25.83	(1 0 2)
44.08	2.053	43.97	43.76	2.068	45.25	(1 1 0)
48.21	1.886	24.41	47.92	1.892	45.29	(1 0 3)
52.18	1.751	39.21	51.92	1.761	15.27	(1 1 2)

Fig. 4. W-H plot for CdS nanoparticles.

edge toward the lower wavelength side, i.e. blue shift in absorption spectra. The absorption spectrum (Fig. 5) displays a decrease in absorption by CdS nanoparticles with the increase in wavelength. It has been found that optical absorption is < 20 % in the visible region indicating high transparency of CdS nanoparticles. In various nanoform of semiconductors an excitation peak exists along with absorption edge [31, 32] which is estimated by the second derivative of absorption spectrum (Fig. 5). In the present study the excitation peak is found at 290 nm and for absorption edge at 460 nm. Oliveira et al. [15] has also reported wurtzite CdS nanoparticles (yellow to orange color) having an absorption edge between 400 nm to 470 nm. The position of the absorption edge has been observed to be blue shifted, by 53 nm relative to the fundamental absorption edge of bulk wurtzite CdS (513.6 nm) [6].

This blue shift in the absorption edge is believed to be caused by the quantum confinement effect which is expected in the nano-sized CdS particles [6]. The particle size and optical band gap values for CdS in various nanoforms have a wide range depending on the synthesis technique. In this study the optical band gap of CdS nanoparticles is calculated to be 2.69 eV.
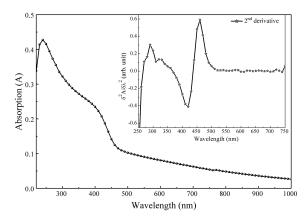

Fig. 5. UV-Vis-NIR absorption spectrum; the inset shows specific energy range second derivative of absorption spectrum.

4. Conclusion

In this work we have synthesized orange color CdS nanoparticles (inset Fig. 2) via co-precipitation technique. The homogeneous precipitation resulted in the cluster growth of CdS nanoparticles. These nanoparticles are polycrystalline in nature having stable (wurtzite) structure with the preferential orientation in (0 0 2) plane.

A Cd–S bond stretching has been identified by absorption peak at 651.62 cm^{-1}. Williamson-Hall (W-H) method has been employed to evaluate particle size (15.23 nm) and microstrain (6.93×10^{-3}). The particle size, analyzed using ImageJ programme is close to that obtained by W-H method. The lattice constants are found to be slightly less than bulk CdS values indicating lattice contraction. The existence of excitation peak and blue shift of fundamental absorption edge indicate quantum size effect in the CdS nanoparticles. These stable phase CdS nanoparticles with enhanced structural and optical characteristics will be more suitable for visible range optoelectronic applications.

References

[1] DEMMING A., *Nanotechnology*, 22 (2011), 090201.

[2] KIM D.H., LU N., GHAFFARI R., ROGERS J.A., *NPG Asia Mater.*, 4 (2012), e15.

[3] CHEN L., JIANG Y., WANG C., LIU X., CHEN Y., JIE J., *J. Exp. Nanosci.*, 5 (2010), 106.

[4] CAO G., *Nanostructures & nanomaterials: synthesis, properties & applications*, Imperial College Press, London, 2004.

[5] SMITH A.M., NIE S., *Accounts Chem. Res.*, 16 (2010), 190.

[6] TAI G., ZHOU J., GUO W., *Nanotechnology*, 21 (2010), 175601.

[7] YAO W.T., YU S.H., *Adv. Funct. Mater.*, 18 (2008), 3357.

[8] JIE J., ZHANG W., BELLO I., LEE C.S., LEE S.T., *Nano Today*, 5 (2010), 313.

[9] KUMAR S., SHARMA P., SHARMA V., *J. Appl. Phys.*, 111 (2012), 113510.

[10] HULLAVARAD N.V., HULLAVARAD S.S., KARULKAR P.C., *J. Nanosci. Nanotechno.*, 8 (2008), 3272.

[11] ZHAI T., FANG X., LI L., BANDO Y., GOLBERG D., *Nanoscale*, 2 (2010), 168.

[12] LI H., WANG X., XU J., ZHANG Q., BANDO Y., GOLBERG D., MA Y., ZHAI T., *Adv. Mater.*, 11 (2013), 3017.

[13] AMCSD (database code - 0015177 and 0011517).

[14] CHEN Q., BAO H., SHEN X., *Phase Transit.*, 81 (2008), 591.

[15] OLIVEIRA J.F.A., MILAO T.M., ARAUJO V.D., MOREIRA M.L., LONGO E., BERNARDI M.I.B., *J. Alloy. Compd.*, 509 (2011), 6880.

[16] BAROTE M.A., YADAV A.A., MASUMDAR E.U., *Physica B*, 406 (2011), 1865.

[17] CABANA Z.L., TORRES C.M.S., GONZALEZ G., *Nanoscale Res. Lett.*, 6 (2011), 523.

[18] PAZ M.G.S., BON R.R., *Thin Solid Films*, 520 (2011), 999.

[19] JUNG D.R., KIM J., NAM S., NAHM C., CHOI H., KIM J.I., LEE J., KIM C., PARK B., *Appl. Phys. Lett.*, 99 (2011), 041906.

[20] CHU J., JIN Z., CAI S., YANG J., HONG Z., *Thin Solid Films*, 520 (2012), 1826.

[21] MONDAL B., SAHA S.K., *J. Nanopart. Res.*, 14 (2012), 1049.

[22] LIU S., YANG M.Q., TANG Z.R., XU Y.J., *Nanoscale*, 7 (2014), 7193.

[23] KRIPAL R., GUPTA A.K., MISHRA S.K., SRIVASTAVA R.K., PANDEY A.C., PRAKASH S.G., *Spectrochim. Acta A*, 76 (2010), 523.

[24] SCHNEIDER C.A., RASBAND W.S., ELICEIRI K.W., *Nat. Methods*, 9 (2012), 671.

[25] BHANDARI K.P., ROLAND P.J., KINNER T., CAO Y., CHOI H., JEONG S., ELLINGSON R.J., *J. Mater. Chem. A*, 3 (2015), 853.

[26] KUMAR S., SHARMA P., SHARMA V., *IEEE T. Nanotechnol.*, 13 (2014), 343.

[27] AMCSD (database code - 0012941).

[28] KALE R.B., LOKHANDE C.D., *Semicond. Sci. Tech.*, 20 (2005), 1.

[29] KUMAR S., SHARMA P., SHARMA V., *Electron. Mater. Lett.*, 9 (2013), 371.

[30] BRUS L., *J. Phys. Chem.*, 90 (1986), 2555.

[31] KATSIKAS L., EYCHMIILLER A., GIERSIG M., WELLER H., *Chem. Phys. Lett.*, 172 (1990), 201.

[32] ACOSTA M.F., LERMA M.S., CHAVEZ H.A., BARRAZA F.F.C., BON R.R., *Solid State Commun.*, 128 (2003), 407.